APEC Climate Center Research Report 2017-03

Development of APCC-PAGASA Regional Prediction System (APCC-PRePS) over the Philippines Year 1: Model Intercomparison

Yoo-Bin Yhang, Chang-Mook Lim, WonMoo Kim Climate Research Team

APCC
APEC CLIMATE CENTER

발간사

계절 예보는 국가의 정책을 결정하는 데 있어 중요한 정보이며, 고해상도의 신뢰도 높은 계절 예측 정보의 중요성이 높아지고 있다. 세계 여러 현업 기관에서 전지구 모형을 이용하여 계절 예측 정보를 생산하고 있지만 기후연구는 물론 수자원, 농업과 같은 응용연구에서 필요로 하는 지역적 특성이 고려된 예측 정보가 부족하며, 악기상과 같은 기상 이변에 대한 예측력은 높지 않은 것으로 알려져 있다.

컴퓨팅 소스의 발달로 모형의 적분 시간이 단축되고 있음에도 불구하고 지역기후모형을 이용한 계절예측정보의 생산은 시간 대비 예측성을 담보하기 힘들다는 이유로 잘 이루어지지 않고 있다. 대부분의 기관에서 과거 자료를 바탕으로 찾아낸 경험식을 이용한 통계적 기법을 통해 예측자료를 생산하고 있으나 통계모형을 통한 예측 역시 역학모형의 예측력이 담보되어야 하는 것이므로, 역학모형의 예측성 향상과 검증이 선행되어야 한다.

필리핀과 같은 개발도상국에서는 컴퓨팅 소스와 같은 하드웨어의 부족 및 기술, 인력의 부족으로 인해 계절예측을 위한 전지구모형의 운영이 어려운 현실이다. APCC와 필리핀 기상청에서는 이러한 현실적인 환경을 고려하여 지역기후모형을 이용한 계절예측 시스템을 구축하는 공동연구를 계획하였다. 본 연구보고서는 공동연구의 첫 번째 단계로, 계절예측시스템에 적용될 지역기후모형 후보군들을 선정하여 모형들의 예측성을 비교·검증하였다. 이 연구 결과를 바탕으로 향후 필리핀 기상청과의 지속적인 논의를 통해 예측성을 검증하고 개선하기 위한 노력이 계속될 것이다.

본 연구보고서가 발간되기까지는 많은 분들의 도움이 있었다. 보고서의 수준을 제고하도록 좋은 논평을 해주신 익명의 검토자들과 연구가 순조롭게 진행될 수 있도록 다방면으로 도와준 임창묵 연구원과 김원무 박사, 그리고 본 연구보고서를 총괄하고 최종집필한 본원의 양유빈 박사에게도 감사의 뜻을 전한다. 본 연구보고서가 밑거름이 되어 향후 관련 연구들이 지속되고 부족한 부분들을 계속 채워나가길 바란다.

2018년 3월
APEC 기후센터
원장 **정 홍 상**

ABSTRACT

This study is a part of the APCC-PAGASA Regional Prediction System (APCC-PRePS) project, aimed at providing valuable high-resolution seasonal forecasts using downscaling techniques. In the first year of the APCC-PRePS project, the purpose of this study is to evaluate the performance of regional climate models and investigate their characteristics in simulating the climate of the Philippines. Dynamical downscaling was carried out by the WRF, RegCM, and GRIMs-RMP with the same horizontal resolution and domain for May-June-July-August from 1986 to 2010. The results were evaluated by APHRODITE and ERA-Interim in terms of climatological mean, interannual variability, and ENSO-related features.

On the whole, there is no single model that outperforms the others in all aspects of simulated climate. The results show that the WRF is capable of reproducing the climatological mean with a certain cold bias and spatial distributions of surface temperature. The GRIMs significantly underestimates surface temperature due to a poor representation of topography, but interannual variabilities are reasonably reproduced. Rainfall anomalies in association with ENSO are well captured in the WRF simulations, despite simulated regional circulations that are weaker than observations. On the contrary, the GRIMs shows exaggerated circulations and a slightly northward flow in the low-level wind, resulting in a northward precipitation band. The RegCM simulates erroneous meridional flows, which causes difficulties in reproducing the climate of the Philippines.

CONTENTS

1. INTRODUCTION

The APEC Climate Center (APCC) aims to increase regional prosperity in the Asia-Pacific region by providing the climate information service, seeking to protect lives and property, reduce economic losses, and enhance economic opportunities. APCC utilizes up-to-date scientific knowledge and applies innovative climate prediction techniques to its climate prediction, interdisciplinary research, climate information services, and international cooperation. To this end, APCC's mission and vision are closely connected to the efforts of the Philippine Atmospheric, Geophysical and Astronomical Services Administration (PAGASA) towards disaster risk reduction.

As skillful seasonal forecasts are essential for natural resource management and decision making, producing an accurate and precise high-resolution seasonal forecast is more necessary than ever. Global climate models (GCM) have provided useful climate information in the past, near present, and future, which is important when assessing the potential impact of global climate change. However, GCMs have coarse spatial resolutions, typically ranging from 100 to 250 km, which may be inadequate in representing some regional climate features. Particularly in archipelagic regions like the Philippines, topography, land use, and coastlines need to be properly resolved in the model as these features affect climate on a local scale.

Studies have shown that regional climate models (RCMs) can provide added value to GCMs, especially for areas with complex topography and coastlines (Feser et al. 2011). For the Philippines, RCMs have been used to examine historical climate and downscaled climate projections (e.g., Im et al. 2008; Robertson et al. 2012). For example, the Abdus Salam International Centre for Theoretical Physics Regional Climate Model version 3 (RegCM3) was used to examine the summer monsoon precipitation over the country and model sensitivity to lateral boundary conditions and ocean flux schemes (Francisco et al. 2006). In addition, the UK Met Office Hadley Centre Providing Regional Climates for Impacts Studies (PRECIS) model and the Weather Research and Forecasting (WRF) model have been used to project future changes in temperature and rainfall over the Philippines and in Southeast

Asia (PAGASA 2011; Chotamonsak et al. 2011). Cruz et al. (2016) evaluated the performance of the non-hydrostatic regional climate model (NHRCM) over the Philippines and investigated the sensitivity to boundary conditions and convective schemes.

Previous RCM studies on the Philippine climate have been limited to climate projection or reproduction. The final goal of the APCC-PAGASA Regional Prediction System (APCC-PRePS) project is to provide valuable high-resolution seasonal forecasts using downscaling techniques. The plan is for the APCC-PRePS project to be conducted over three years, from 2017 to 2019. In the first year of the APCC-PRePS project, we conduct an intercomparison of regional climate models. RCMs have their own characteristics due to varying dynamics and physical processes. Therefore, it is necessary to investigate the performance of regional climate models over the Philippines. This study is the first step in choosing an RCM for operational use in the future. The purpose of this study is to evaluate the performance of the regional models and investigate their characteristics in simulating the climate of the Philippines.

Details on the APCC-PRePS project are given in the next section. In section 3, we present data and methodology, section 4 provides results from three regional climate models, and in section 5 we summarize and discuss the results. Finally, future plans are provided in section 6.

2. APCC-PRePS PROJECT

The ultimate goal of this project is to increase the reliability of action plans against possible climate-induced risks in the Philippines by delivering more detailed seasonal prediction information. This will be achieved through the building and installation of a downscaling system on the PAGASA supercomputer.

The APCC-PRePS project, scheduled for 3 years, consists of four steps, as shown in Figure 1.

Strategic plans for each year are shown below.

- 1st year:
  - Analyze the characteristics of regional climate models over the Philippines
  - Intercompare the predictability of regional climate models
  - Select the best model for the prediction system
- 2nd year:
  - Perform sensitivity tests to boundary conditions, domains, and physics using the selected model
  - Investigate predictability
  - Decide model configuration considering practical and operational aspects
- 3rd year:
  - Produce hindcast
  - Evaluate hindcast
  - Test operation
  - Run the operational system

3. DATA AND METHODOLOGY

3.1 Models

We selected three regional climate models as candidates for the seasonal forecast system—WRF, GRIMs, and RegCM—for intercomparison of simulations over the Philippines. These models are flexible, easily accessible, and easy to use. Also, previous studies have demonstrated their predictability over various regions.

The Weather Research and Forecasting (WRF) model v3.8, released in April 2016, was used in this study. The WRF employs fully compressible non-hydrostatic equations with hydrostatic options, and WRF v3.3 has been used for numerical weather prediction at PAGASA. It is developed as a collaborative effort among several universities and federal research agencies in the USA. It is the next generation of the PSU/NCAR fifth generation mesoscale model, known as MM5 (Chen and Dudhia 2001; Barker et al. 2004; Ishak et al. 2013). The WRF has significant improvement over the MM5 and includes recent physics parameterizations. The WRF is designed to serve and support both atmospheric research and operational forecasting needs (Dai et al. 2013; Islam et al. 2013; Srivastava et al. 2013a, b; Islam et al. 2014).

The Global/Regional Integrated Model System (GRIMs; Hong et al. 2013) has been created for numerical weather prediction, seasonal simulation, and climate research projects, from global to regional scales. The primary version of global and regional models is rooted in the NCEP seasonal forecast model (Kanamitsu et al. 2002) and regional spectral model (Juang et al. 1997), but with subsequent developments of model physics and dynamics, along with the re-configuration of code structure. The model system is developed and practiced by taking advantage of both operational and research applications. The regional part of the GRIMs, namely RMP (hereafter GRIMs-RMP), has been successfully employed as a tool to better understand the precipitation mechanisms of the Asian monsoon (Koo and Hong 2010; Hong et al. 2012).

The latest version of the International Centre for Theoretical Physics (ICTP) regional climate model, RegCM4 (Giorgi et al. 2012), is an upgrade of the model originally developed by Giorgi et al. (1993a, 1993b) and Pal et al. (2007). RegCM4 is a hydrostatic, compressible, and sigma-p vertical coordinate model. A time-splitting explicit integration scheme is used, in which the two fastest gravity modes are first separated from the model solution and then integrated with smaller time steps. This allows the use of a longer time step for the rest of the model. Essentially, the model dynamics is the same as that of the hydrostatic version of MM5.

3.2 Experimental Design

Dynamical downscaling is carried out by the WRF, GRIMs-RMP, and RegCM with the same horizontal resolution and domain. Three sets of regional model simulations were made over the maritime continent, focusing on the Philippines (Figure 2a) with a 20-km grid resolution to resolve the forcing by local mountains and coastlines. The models were driven by the NOAA optimally-interpolated sea surface temperature (SST) analysis (Reynolds et al. 2002) within the model domain (approximately 11 °S – 30 °N, 94 °E – 152 °E) and six-hourly fields from the National Centers for Environmental Prediction (NCEP) Climate Forecast System Reanalysis (CFSR; Saha et al. 2010) as boundary conditions. Experimental designs for the three regional models are shown in Table 1. The experiments were conducted during the rainy season (May-June-July-August) from 1986 to 2010 to examine the applicability of the RCMs in the Philippines.

For the model evaluation, gridded observation datasets have been used to overcome limitations posed by sparse meteorological stations and missing data. Simulated precipitation and surface temperatures obtained from experiments are compared with the Asian Precipitation–Highly Resolved Observational Data Integration Towards Evaluation (APHRODITE; Yasutomi et al. 2011). These datasets are based on station records as well as pre-compiled datasets, and are only available over land. The APHRODITE provides a detailed distribution of precipitation with higher spatial and temporal resolutions (0.25°×0.25° and daily, respectively). Since the APHRODITE dataset ends in December 2007, the time period for the analysis of model results is set to 22 years, from 1986 to 2007. For evaluation, basic statistics such as temporal and spatial correlation are tabulated against the APHRODITE data. To facilitate the validation of the simulated large-scale circulation by the RCMs, ECMWF ERA-Interim (Dee et al. 2011) is used.

4. RESEARCH RESULTS

In this section, the simulated features from the WRF, GRIMs-RMP, and RegCM are intercompared and evaluated.

4.1 Climatological Features and Mean Biases

The simulated climate is compared to observations in terms of climatological mean. The Philippines is a region close to the Asiatic mainland. Archipelagic in nature, it is subdivided into three geographic regions: Luzon, Visayas, and Mindanao. The climate of the place is predominantly controlled by topography, with several islands, mountain ranges, and coastal plains; wind systems result from the seasonal differential heating of neighboring continents and oceans. Rainfall activity over the place was mainly due to mesoscale phenomena, such as rainbelts associated with the intertropical convergence zone (ITCZ), the tail end of the cold front, the northeast monsoon (locally known as 'Amihan'), the southwest monsoon (locally known as 'Habagat'), semi-permanent high-pressure systems, and tropical cyclones (Jose et al. 2002). Generally, its climate can be described as humid equatorial, with marked high temperatures but with slight differences between maximum and minimum temperatures, and tropical maritime, with uneven rainfall distribution throughout the year and noticeable high annual rainfall.

Figure 3 shows seasonal mean large-scale circulations. The southwest monsoon, or summer monsoon, commences from the Australian anticyclone during the southern hemisphere winter. This migrating tropical air mass generally arrives at the Philippines from the southwesterly direction as illustrated in Figure 3a. The southwest monsoon brings heavy rains, which are concentrated over the western coastal areas of Luzon and the Visayas. Thus, aside from tropical cyclones, it is responsible for a great portion of the rainfall during the rainy season. The WRF overestimates sea level pressure and temperature at 850 hPa, which results in weak southwesterlies (Figure 3b). In the GRIMs runs, slightly stronger pressure and lower temperature is presented (Figure 3c). The RegCM overestimates pressure and underestimates temperature over the domain (Figure 3d).

To compare the mean biases of the models, root mean square errors (RMSEs) of large-scale circulation are calculated over the experimental domain (Figure 4). Differences between CFSR and ERA-Interim are also represented to determine the effect of boundary conditions on simulated fields. The GRIMs shows a similar profile as the CFSR, resulting in the smallest biases, with the exception of temperature. Since a spectral nudging method is applied to the zonal and meridional wind in the GRIMs runs, it can influence performance of the model. In the RegCM runs, errors grow according to vertical level in height and wind (Figures 4b - 4d). In particular, the error in the meridional wind is much larger than the other two models (Figure 4d).

The climate of the Philippines is described as tropical and maritime. During the summer season from June to August, the temperature over the country averages about 28°C with lower temperatures over the mountainous areas in northwest of Luzon island and the western section of Mindanao island (Figure 5a). Three regional models tend to underestimate temperature (Figures 5b-5d). Particularly, negative bias is most significant in the GRIMs (Figure 5c) due to differences in height between actual and model elevations. Compared to the WRF and RegCM, terrain heights in the GRIMs are lower (not shown), which affects the simulated temperature, e.g., higher temperature over the mountains. Since topography represented in the model is not as sophisticated as actual geographical features, the model does not resolve plain-mountain contrast. While the model temperature is lower over basins surrounded by mountains, the model overestimates temperature over mountainous areas. Therefore, it is necessary to adjust the model values (over land points only) using a temperature lapse rate of 6°C km^{-1}, similar to APHRODITE (Yasutomi et al. 2011), to provide real values of surface temperatures.

The seasonal and spatial variability in the Philippine climate is mainly driven by rainfall, which is influenced by both local processes and large-scale systems, e.g., the northeast and southwest monsoons, tropical cyclones, and the El Niño Southern Oscillation (Cruz et al. 2013; Villafuerte et al. 2014). In summer, the southwest monsoon brings abundant rainfall over the western coast, particularly over northwest Luzon, while the rest of the country receives at least 5 mm day^{-1} (Figure 6a). Three regional models capture the southwest monsoon and its associated high rainfall along the western coastline. However, all models tend to underestimate rainfall in Luzon and Visayas due to weaker monsoonal flow (Figures 6b–6d).

4.2 Interannual Variability

In this section, we analyze the performance of three regional climate models to capture the yearly variation in surface temperature and precipitation for each month during summer.

Figure 7 presents the temporal evolution of temperature anomalies to measure the interannual variability of the observed and simulated temperature over the Philippines. Regardless of the land surface model applied to the model simulation, all regional climate models simulate similar trends in each month of June, July, and August. It results in similar correlation values for those months. While neither model follows the observed trend in May (Figure 7a), the simulated temperature anomalies show similar evolution in June and July (Figures 7b and 7c).

To examine the spatial distribution of temporal correlation coefficients, temporal correlations are represented at each grid point in Figure 8. It is found that the most predictive regions are the southern parts of Luzon and Visayas. All of three models exhibit the highest correlation in July. Temporal correlations for June and July for 22 summers are larger than the p-value of the 95% significance level.

We investigate how well the spatial distribution of simulated temperatures matches the observation in terms of the correlation, RMSE, and the ratio of variance. The results are shown as a Taylor diagram in Figure 9. Spatial correlation coefficients and standard deviations are calculated in each year from 1986 to 2007. Normalized standard deviations of the models are represented by the ratio to the observation. The WRF runs (blue circle) have similar variation to the observation. The GRIMs (orange) shows relatively low variation compared to the WRF and GRIMs simulations. The GRIMs and RegCM (green) runs exhibit a similar correlation of about 0.8 (Figures 9b-9d). The WRF simulations show the highest correlation of about 0.9 and the lowest RMSE.

We compare precipitation anomalies of observation and three regional climate models in Figure 10. Compared with the results from the other models, precipitation anomalies simulated by the GRIMs follow observed trends except for July (Figures 10c and 10e). Although the RegCM yields the best correlation value for July (Figure 10c), it shows the lowest skill score for other months (Figure 10e). The correlation of the WRF ranges from 0.1 and 0.2.

Compared with temperature, the temporal correlation of precipitation between the model simulation and the observation is lower (Figure 11). The WRF has better skill in the northern part of Luzon than in other regions, but it is not statistically significant (Figure 11a). The GRIMs shows a high average correlation in Luzon and Visayas (Figure 11b). In May, high correlation values exceeding the 95% confidence level (0.44) are evident in the Philippines. The RegCM gives the lowest rainfall anomaly correlation in May, June, and August (Figure 11c).

In terms of rainfall amount, the WRF exhibits the best performance (Figure 12a). Although the GRIMs represents the best temporal correlation skills, RMSE is higher than the other two models (Figure 12b). It indicates that the model follows interannual variability, but does not capture the amount of precipitation. Errors are evident over the mountains in west Luzon and Mindanao, which are related to the poor representation of topography in the GRIMs. The RegCM has large biases along the west coast in Luzon (Figure 12c).

Spatial correlations and RMSE for simulated precipitation are not as high as those for temperature (Figure 13). In several years, regional models show negative correlations. The models show large variance in May but small variance in August. All models show poor performance in July. Generally, the WRF runs show relatively small variance and small RMSE compared to the other models.

4.3 ENSO-Related Features

In this section, we investigate the performance of the model to simulate the effect of El Niño Southern Oscillation. El Niño Southern Oscillation (ENSO) is the most important source of interannual variability of rainfall in the Philippines and in many other areas of the world (Ropelewski and Halpert 1987; Allen et al. 1996). The role of ENSO has influenced world history, and the association of warm episodes in the Pacific Ocean and drought in the Philippines has been documented since the mid-1980s (Jose 1989, 1990). While ENSO amplifies the variability, it also provides predictability for this variability, which may be used in risk management. ENSO-based forecasts can help people in regions affected by ENSO to be more prepared and cope better with ENSO-related climate variability (Hansen 2002; Jose 2002; Meinke et al. 2003).

The extreme phases of the ENSO phenomenon have a strong modulating effect on seasonal rainfall in the Philippines, with mature ENSO warm events (El Niño) often associated with drought and stresses on water resources and agriculture, while cold events (La Niña) often result in excessive rainfall (Jose 2002; Lyon et al. 2006). However, a number of sites in north-central Philippines show a summer reversal in the ENSO rainfall signal (Lyon and Camargo 2009), in which wetter than normal conditions persist during July to September, before the drier than normal conditions in the later months of the year and the following year, associated with El Niño. The reverse is true during La Niña years. Therefore, changes in precipitation and associated circulation during July and August (JA) is analyzed in this section.

The EN (El Niño) and LN (La Niña) events were identified using SST anomalies averaged over the Niño 3.4 region (5 °S – 5 °N, 120 °W – 170 °W; Barnston et al. 1997), obtained from http://origin.cpc.ncep.noaa.gov/products/analysis_monitoring/ensostuff/ONI_v5.php. As a starting point, the observed precipitation data for JA (July-August) during the 5 EN (1987, 1991, 1997, 2002, 2004) and 4 LN (1988, 1998, 1999, 2000) events between 1986 and 2007 were used to identify regions with statistically significant rainfall anomalies across the Philippines (Figure 14). A significant occurrence of above (below) average rainfall is seen under EN (LN) conditions in the north-central Philippines (boxed region in Figure 14a, land areas only), in agreement with previous results (Figure 14a). The WRF and RegCM simulate the wet anomaly in the north-central Philippines in EN years (Figures 14b and 14d), whereas the GRIMs shows dry conditions (Figure 14c). In LN years, three models present negative anomalies in the north-central regions. Thus, the wetter conditions in north-central Philippines are significant in the composite difference of the WRF runs (Figure 14b). Although the GRIMs simulates wet conditions in the Bicol region at a 95% confidence level, it demonstrates dry conditions in western Visayas due to an underestimation of precipitation in EN years (Figure 14c). The RegCM shows wetter conditions in the composite difference, but the difference is not statistically significant (Figure 14d).

The monsoon trough is an important contributor to summer rainfall in the Philippines. Previous studies have indicated that the western North Pacific monsoon trough tends to be enhanced and extends southeastward during the onset phase of EN events (Lander 1994; Wang and Zhang 2002; Lau and Nath 2006). Figure 15 shows the climatological mean location of the monsoon trough in July based on the relative vorticity at 850 hPa. The trough extends from the South China Sea eastward across the northern Philippines, then southeastward across the Philippine Sea (Figure 15a). The change in intensity of the monsoon trough across the Philippines and western North Pacific of both EN and LN years is found to primarily result from changes in the zonal component of the low-level wind. That is,

$$\delta' = \frac{\partial u'}{\partial y}$$

the anomalous relative vorticity at 850 hPa is approximately equal to the meridional gradient of the anomalous zonal wind (Lyon and Camargo. 2009). Thus, primary remote forcing to the Philippines is associated with an anomalous cyclonic (anticyclonic) circulation over the western North Pacific during JA of EN (LN) years. A band of anomalous westerlies (easterlies) across the WNP increases (decreases) the monsoon flow across the north-central Philippines, while the horizontal shear of this flow is associated with a deepened (weakened) monsoon trough. The trough is weakened (strengthened) in the vicinity of the Philippines during the fall of EN (LN) events, which also indicates a departure from the zonally-elongated banded structure seen in July as the anomalous anticyclone (cyclone) develops over the Philippines during EN (LN). These features help explain why the reversal in the ENSO rainfall signal is confined to the relatively narrow region of the north-central Philippines.

Consistent with previous studies (Wu et al. 2003; Wang et al. 2003; Juneng and Tangang 2005), the composite anomalies for EN years shows an anomalous cyclonic circulation centered east of the Philippines near 15 °N with anomalous, largely off-equatorial, low-level westerlies extending from the Indochina Peninsula eastward over the Philippines (Figure 15a). These anomalies indicate an enhancement of the summer monsoon flow over the central Philippines, favoring increased rainfall given a substantial interaction of the low-level flow with local topography in the region (Chang et al. 2005). In LN years, the pattern is generally opposite that of the EN composite with anomalous easterlies over the central and southern Philippines opposing the zonal component of the monsoon flow.

The WRF produces a similar location for the monsoon trough as the ERA-Interim, which extends from the South China Sea to northern Philippines (Figure 15b). While the observed trough extends southeastward across the north-central Philippines, the simulated trough extends slightly northeastward. In EN years, the cyclonic circulation is well captured, but the positive core is located around 10 °N. In the GRIMs simulation, a band of positive relative vorticity is not significant as in the observation, but extends southeastward (Figure 15c). For EN years, the center of the positive relative vorticity is not clear, which results in weak cyclonic circulation. This is related to underestimation of precipitation in western Visayas in EN years (see Figure 14c). Though the WRF (GRIMs) underestimates (overestimates) negative relative vorticity in LN years, both models well capture anticyclonic circulation over the Philippine Sea (Figures 15b and 15c). The RegCM shows a very weak trough in the climatological field (Figure 15d), and it fails to simulate the anomalous circulations in both EN and LN years.

Previous work has shown that over the north-central Philippines, the total moisture flux tends to be enhanced (reduced) in July to September of EN (LN) years (Juneng and Tangang 2005; Lyon et al. 2006). The horizontal wind vector V and specific humidity q at 850 hPa were decomposed as the sum of the climatological mean and anomalous components. The anomalous moisture flux may be written as the sum of three terms,

$$(qV)_a = q_c V_a + q_a V_c + (q_a V_a)_a \qquad (1)$$

where the subscripts a and c denote the anomalous and climatological values, respectively.

The first term on the right-hand side of Eq. (1), the anomalous 850-hPa wind (V_a) acting on the climatological specific humidity field (q_c), is by far the main contributor of the total anomalous flux (Figure 16). In July of EN years, a band of enhanced westerly moisture flux centered north of the equator extends from the South China Sea across the central Philippines to the tropical Western North Pacific (Figure 16a). A generally opposite pattern with reversed direction is seen for the composite LN. Both the WRF and GRIMs reproduce a band of enhanced westerly moisture flux in EN years and reversed flow in LN years (Figures 16b and 16c). On the other hand, the RegCM shows unusual southerlies in EN and northerlies in LN years (Figure 16d).

The second term in Eq. (1), the contribution of anomalous specific humidity (q_a) on the moisture flux by the climatological wind (V_c) has a much smaller magnitude than the first term (Figure 17). It reinforces the first term across the central Philippines during both EN and LN years (Figure 17a). This result indicates that the enhanced (reduced) monsoon flow across the central Philippines during JA of EN (LN) years also has slightly higher (lower) moisture content than the climatological mean. This is consistent with the sign of the rainfall anomalies shown in Figure 15, although this analysis cannot discern causality (e.g., increased rainfall in JA of EN years would serve to moisten the atmosphere in its own right). Compared to observations, the contribution of the anomalous specific humidity on the moisture flux by the climatological wind is not significant in the WRF simulation in neither EN nor LN years (Figure 17b). In the GRIMs simulation, the reinforcement by the second term in Eq. (1) is distinct over the South China Sea both in EN and LN years (Figure 17c). However, the enhanced monsoon flow is located westward, compared to observations, resulting in overestimated (underestimated) precipitation over northern Luzon in EN (LN) years (See Figure 14c). The RegCM simulates very erroneous flow both in EN and LN years (Figure 17d), which is related to large RMSE in the meridional wind (See Figure 4d).

The last term in Eq. (1), the anomalous eddy moisture flux ($q_a V_a$), does not significantly contribute to the anomalous flux during JA, being considerably smaller than the second term (not shown). Overall, this analysis indicates the primary role of the anomalous low-level wind field in determining moisture flux changes across the Philippines during ENSO events. Similar to the wind field anomalies in Figure 15, the largest anomalies in the 850-hPa moisture flux are generally located over the central Philippines.

5. SUMMARY AND DISCUSSION

This study was performed as the first step of the APCC-PAGASA Regional Prediction System (APCC-PRePS) project. The final goal of the APCC-PRePS project is to provide valuable high-resolution seasonal forecasts using downscaling techniques. In this year, we conducted an intercomparison of regional climate models to evaluate the performance of the models and investigate their characteristics in simulating the climate of the Philippines. We selected three regional climate models as candidates for the seasonal forecast system: WRF, GRIMs, and RegCM. Three sets of regional model simulations were made over the maritime continent, focusing on the Philippines with a 20-km grid resolution. The models were driven by the NOAA optimally-interpolated sea surface temperature (SST) analysis and six-hourly fields from the National Centers for Environmental Prediction (NCEP) Climate Forecast System Reanalysis (CFSR) as boundary conditions. The experiments were conducted during the rainy season (May-June-July-August) from 1986 to 2010 to examine the applicability of the RCMs in the Philippines.

The simulated features from the WRF, GRIMs-RMP, and RegCM were intercompared and evaluated in terms of climatological mean, interannual variation, and ENSO-related features. Overall, the GRIMs reproduced large-scale features. This is expected because a spectral nudging technique (Hong and Chang 2012) is applied only in the GRIMs simulation. The application of spectral nudging permits the retention of large-scale information resolved by the global model (or reanalysis) in the regional model. The regional model can add smaller-scale information to the large-scale solution. Although all models showed a cold bias in the Philippines, simulated temperature by the WRF was the closest to the observation. The common biases in the simulated precipitation were the underestimation in Luzon and overestimation in Mindanao.

The simulated surface temperatures agreed reasonably well with observed trends in each month except for May. Similar to the climatological mean, the WRF well reproduced the spatial pattern of temperature with the smallest RMSE. The biases in the simulated precipitation were larger than temperature. In the GRIMs run, the interannual variability of monthly precipitation averaged over the Philippines agreed well with observations for most months, and predictive regions with statistical significance were relatively distinct from the other models. However, notable errors were shown in the mountainous regions, related to the poor representation of topography in the GRIMs.

The ENSO-related variations in summer precipitation and regional circulation were also analyzed. All models reproduced the features in the La Niña years than those in the El Niño years. The WRF simulated wet conditions over the north-central Philippines in the El Niño years, which results in significant differences between El Niño and La Niña events. The anomalous low-level wind response across the western north Pacific plays a role in increasing (decreasing) the moisture flux into the north-central Philippines during July-August in the El Niño (La Niña) years. This flow was well simulated in the WRF runs. The GRIMs also presented these regional circulations, but simulated locations were slightly shifted. Therefore, the associated rainfall anomalies moved northward. The RegCM simulations showed erroneous flow both in El Niño and La Niña years, and failed to capture these anomalous circulations.

On the whole, each model has advantages and disadvantages in reproducing the climate over the Philippines. Selecting the best model that outperforms the others is difficult. Nevertheless, we can suggest the following:

1) The WRF shows relatively better performance in simulating the absolute value (not anomaly) of surface temperature and precipitation.

2) The GRIMs shows relatively better performance in reproducing the interannual variability of surface temperature and precipitation. However, GRIMs runs show deficiencies due to poor representation of topography.

3) The RegCM shows erroneous flow in low level. If we want to use the model in the prediction system, we have to check the associated large-scale circulations.

6. FUTURE PLANS

APCC and PAGASA plan to have a meeting every year during this project. In the next meeting, we will choose the model for the seasonal prediction system based on the results of this year. We must consider the most expected components for seasonal forecast in the Philippines (e.g., intensity, frequency, amount, onset/offset).

The next step of the APCC-PRePS project is to optimize and deliver the downscaling system for seasonal prediction. To do that, we will conduct a sensitivity test using a selected model. We are designing several experiments to consider aspects such as boundary forcing, ensemble method, domain, and resolution. We will discuss this detailed plan with PAGASA.

REFERENCES

Antic S, R. Laprise, B. Denis, and R. de Elía, 2004: Testing the downscaling ability of a one-way nested regional climate model in regions of complex topography. *Clim. Dyn.*, **23**, 473-493.

Barnston A.G., M. Chelliah, and S. B. Goldenberg, 1997: Documentation of a highly ENSO-related SST region in the equatorial Pacific. *Atmos. Ocean*, **35**, 367-383.

Barker, D.M., W. Huang, Y. R. Guo, A. J. Bourgeois, and Q. N. Xiao, 2004: A three-dimensional variational data assimilation system for MM5: implementation and initial results. *Mon. Wea. Rev.,* **132**, 897-914.

Byun, Y. H., and S.-Y. Hong, 2007: Improvements in the subgrid-scale representation of moist convection in a cumulus parameterization scheme: The single-column test and its impact on seasonal prediction. *Mon. Wea. Rev.,* **135**, 2135-2154.

Chang, C.-P., Z. Wang, J. McBride, and C.-H. Liu, 2005: Annual cycle of Southeast Asia—maritime continent rainfall and the asymmetric monsoon transition. *J Climate*, **18**, 287-301.

Chen, F, and J. Dudhia, 2001: Coupling an advanced land surface-hydrology model with the Penn State-NCAR MM5 modeling system. Part I: model implementation and sensitivity. *Mon. Wea. Rev.*, **129**, 569-585.

Chotamonsak, C., E. P. Salathé, Jr., J. Kreasuwan, S. Chantara, and K. Siriwitayakom, 2011: Projected climate change over Southeast Asia simulated using a WRF regional climate model. *Atmos. Sci. Lett.*, **12**, 213-219.

Cruz, F. T., G. T. Narisma, M. Q. Villafuerte II, K. U. Cheng Chua, and L. M. Olaguera, 2013: A climatological analysis of the southwest monsoon rainfall in the Philippines. *Atmos. Res.*, **122**, 609-616.

______, H. Sasaki, and G. T. Narisma, 2016: Assessing the sensitivity of the Non-Hydrostatic Regional Climate Model to boundary conditions and convective schemes over the Philippines. *J. Meteor. Soc. Japan*, **94A**, 165-179.

Dai, Q, D. W. Han, M. A. Rico-Ramirez, and T. Islam, 2013: The impact of raindrop drift in a three-dimensional wind field on a radar-gauge rainfall comparison. *Int. J. Remote Sens.,* **34**, 7739-7760.

Dee, D. P., S. M. Uppala, A. J. Simmons, P. Berrisford, P. Poli, S. Kobayashi, U. Andrae, M. A. Balmaseda, G. Balsamo, P. Bauer, P. Bechtold, A. C. M. Beljaars, L. van de

Berg, J. Bidlot, N. Bormann, C. Delsol, R. Dragani, M. Fuentes, A. J. Geer, L. Haimberger, S. B. Healy, H. Hersbach, E. V. Hólm, L. Isaksen, P. Kållberg, M. Köhler, M. Matricardi, A. P. McNally, B. M. Monge-Sanz, J.-J. Morcrette, B.-K. Park, C. Peubey, P. de Rosnay, C. Tavolato, J.-N. Thépaut, and F. Vitart, 2011: The ERA-Interim reanalysis: configuration and performance of the data assimilation system. *Quart. J. Roy. Meteor. Soc.*, **137**, 553-597.

Dickinson, R. E., A. Henderson-Sellers, and P. J. Kennedy, 1993: Biosphere-atmosphere transfer scheme (BATS) version 1E as coupled to the NCAR Community Climate Model. Technical Note NCAR/TN-387+STR.

Ek, M. B., K. E. Mitchell, Y. Lin, E. Rogers, P. Grunmann, V. Koren, G. Gayno, and J. D. Tarpley, 2003: Implementation of Noah land surface model advances in the National Centers for Environmental Prediction operational mesoscale Eta model. *J. Geophys. Res.,* **108,** 8851. doi:10.1029/2002JD003296.

Emanuel, K.A., and M. Zivkovic-Rothman, 1999: Development and evaluation of a convection scheme for use in climate models. *J. Atmos. Sci.*, **56**, 1766-1782.

Feser, F., B. Rockel, H. von Storch, J. Winterfeldt, and M. Zahn, 2011: Regional climate models add value to global model data: A review and selected examples. *Bull. Amer. Meteor. Soc.*, **92**, 1181-1192.

Francisco, R. V., J. Argete, F. Giorgi, J. Pal, X. Bi, and W. J. Gutowski, 2006: Regional model simulation of summer rainfall over the Philippines: Effect of choice of driving fields and ocean flux schemes. *Theor. Appl. Climatol.*, **86**, 215-227.

Giorgi, F., and coauthors, 2012: RegCM4: model description and preliminary tests over multiple CORDEX domains. *Clim. Res.,* **52**, 7-29.

______, M. R. Marinucci, and G. T. Bates, 1993a: Development of a Second-Generation Regional Climate Model (RegCM2). Part I: Boundary-layer and radiative transfer processes. *Mon. Wea. Rev.*, **121**, 2794-2813.

______, ______, G. DeCanio, and G. T. Bates, 1993b: Development of a Second-Generation Regional Climate Model (RegCM2). Part II: Convective processes and assimilation of lateral boundary conditions. *Mon. Wea. Rev.*, **121**, 2814-2832.

Han, J., and H.-L Pan, 2011: Revision of convection and vertical diffusion schemes in the NCEP Global Forecast System. *Wea. Forecasting*, **26**, 520-533.

Hansen, J.W. 2002: Realizing the potential benefits of climate prediction to agriculture: issues, approaches, challenges. *Agricultural Systems,* **74**, 309-330.

Holtslag, A. A. M., E. I. F. De Bruijn, and H. L. Pan, 1990: A high resolution air mass transformation model for short-range weather forecasting. *Mon. Wea. Rev.*, **118**, 1561–1575.

Hong S.-Y., H.-M. H. Juang, and Q. Zhao, 1998: Implementation of prognostic cloud scheme for a regional spectral model. *Mon., Wea. Rev.,* **126**, 2621–2639.

______, J. Dudhia, and S.-H. Chen, 2004: A revised approach to ice microphysical processes for the bulk parameterization of clouds and precipitation. *Mon. Wea. Rev.,* **132**, 103–120.

______, Y. Noh, and J. Dudhia, 2006: A new vertical diffusion package with an explicit treatment of entrainment processes. *Mon. Wea. Rev.*, **134**, 2318–2341. doi:10.1175/MWR3199.1.

______, and E.-C. Chang, 2012: Spectral nudging sensitivity experiments in a regional climate model. *Asia Pac. J. Atmos. Sci.,* **48**, 345–355.

______, H. Park, H.-B. Cheong, J.-E. E. Kim, M.-S. Koo, J. Jang, S. Ham, S.-O., Hwang, B.-K. Park, E.-C. Chang, and H. Li, 2013: The Global/Regional Integrated Model System (GRIMs). *Asia-Pacific J. Atmos. Sci.*, **49**, 219–243.

Im, E.-S., J.-B. Ahn, A. R. Remedio, and W.-T. Kwon, 2008: Sensitivity of the regional climate of East/Southeast Asia to convective parameterizations in the RegCM3 modelling system. Part 1: Focus on the Korean peninsula. *Int. J. Climatol.*, **28**, 1861–1877.

Ishak A, R. Remesan, P. Srivastava, T. Islam, D. W. Han, 2013: Error correction modelling of wind speed through hydro-meteorological parameters and mesoscale model: a hybrid approach. *Water Resour. Manag.,* **27**, 1–23.

Islam T, M. A. Rico-Ramirez, D. W. Han, M. Bray, and P. K. Srivastava, 2013: Fuzzy logic based melting layer recognition from 3 GHz dual polarization radar: appraisal with NWP model and radio sounding observations. *Theor. Appl. Climatol.,* **112**, 317–338.

______, M. A. Rico-Ramirez, D. W. Han, and P. K. Srivastava, 2014: Sensitivity associated with bright band/melting layer location on radar reflectivity correction for attenuation at C-band using differential propagation phase measurements. *Atmos. Res.,* **135**, 143–158. doi:10.1016/j.atmosres.2013.09.003.

Jose, A.M., F. Hilario, and E. Juanillo, 2002: El Niño vulnerability for rice and corn. Quezon City: PAGASA.

Juneng, L., and F. T. Tangang, 2005: Evolution of ENSO-related rainfall anomalies in Southeast Asia region and its relationship with atmosphere-ocean variations in Indo-Pacific sector. *Clim. Dyn.*, **25**, 337–350.

Kanamitsu, M., W. Ebisuzaki, J. Woollen, S.-K. Yang, J. J. Hnilo, M. Fiorino, and G. L. Potter, 2002: NCEP-DOE AMIP-II reanalysis (R-2), *Bull. Amer. Meteor. Soc.*, **83**, 1631-1643.

Lander, M. A., 1994: An exploratory analysis of the relationship between tropical storm formation in the western North Pacific and ENSO. *Mon. Wea. Rev.*, **122**, 636-651.

Lau, N.-C., and M. J. Nath, 2006: ENSO modulation of the interannual and intraseasonal variability of the East Asian monsoon - a model study. *J. Climate*, **19**, 4508-4530.

Lyon, B., H., Cristi, E.R. Verceles, F. D. Hilario, and R. Abastillas. 2006: Seasonal reversal of the ENSO rainfall signal in the Philippines. *Geophys. Res. Lett.*, **33,** L24710, doi:10.1029/2006GL028182.

______, and S. J. Camargo, 2009: The seasonally-varying influence of ENSO on rainfall and tropical cyclone activity in the Philippines. *Clim. Dyn.*, **32**, 1. doi.org/10.1007/s00382-008-0380-z.

Meinke, H., W. Wright, P. Hayman, and D. Stephens. 2003: Managing cropping systems in variable climates. In Principles of field crop production. 4th edition edited by J. Pratley, pp. 26-77. Oxford, UK: Oxford University Press.

PAGASA, 2011: Climate Change in the Philippines. Funded by the MDGF 1656: Strengthening the Philippines' Institutional Capacity to Adapt to Climate Change Project. DOST-PAGASA, 85 pp.

Pal, J. S., E. E. Small, and E. A. B. Eltahir, 2000: Simulation of regional-scale water and energy budgets: representation of subgrid cloud and precipitation processes within RegCM, *J. Geophys. Res.*, **105**, 29579-29594.

______, F. Giorgi, X. Bi, N. Elguindi, F. Solmon, X. Gao, R. Francisco, A. Zakey, J. Winter, M. Ashfaq, F. Syed, J. Bell, N. Diffenbaugh, J. Karmacharya, A. Konare, D. M.-C., R. P. da Rocha, L. Sloan, and A. Steiner, 2007: Regional climate modeling for the developing world: the ICTP RegCM3 and RegCNET. *Bull. Amer. Meteor. Soc.,* **88**, 1395-1409.

Park, H., and S.-Y. Hong, 2007: An evaluation of a mass-flux cumulus parameterization scheme in the KMA global forecast system. *J. Meteor. Soc. Japan*, **85**, 151-169.

Reynolds, R. W., N. A. Rayner et al., 2002: An improved in situ and satellite SST analysis for climate. *J. Climate*, **15**, 1609-1625.

Robertson, A. W., J.-H. Qian, M. K. Tippett, V. Moron, and A. Lucero, 2012: Downscaling of seasonal rainfall over the Philippines: Dynamical versus statistical approaches. *Mon. Wea. Rev.*, **140**, 1204-1218.

Ropelewski, C.F., and M.S. Halpert. 1987: Global and regional scale precipitation patterns associated with the El Niño/Southern Oscillation. *Mon. Wea. Rev.,* **115**, 1606-1626.

Saha, S., et al., 2010: The NCEP Climate Forecast System Reanalysis, *Bull. Amer. Meteor. Soc.*, **91**, 1015–1057, doi:10.1175/2010BAMS3001.1.

Srivastava P. K., D. W. Han, M. A. R. Ramirez, and T. Islam, 2013a: Comparative assessment of evapotranspiration derived from NCEP and ECMWF global datasets through Weather Research and Forecasting model. *Atmos. Sci. Lett.,* **14**, 118–125.

______, D. W. Han, M. A. Rico-Ramirez, D. Al-Shrafany, and T. Islam, 2013b: Data fusion techniques for improving soil moisture deficit using SMOS satellite and WRF-NOAH land surface model. *Water Resour. Manag.*, **27**, 5069–5087.

Villafuerte, M. Q., J. Matsumoto, I. Akasaka, H. G. Takahashi, H. Kubota, and T. A. Cinco, 2014: Long-term trends and variability of rainfall extremes in the Philippines. *Atmos. Res.*, **137**, 1-13.

Wang, B., and Q. Zhang, 2002: Pacific-East Asian teleconnection. Part II: how the Philippines Sea anomalous anticyclone is established during El Niño development. *J. Climate*, **15**, 3252–3265.

______, R. Wu, and T. Li, 2003: Atmosphere–Warm Ocean interaction and its impacts on Asian–Australian Monsoon Variation. *J. Climate*, **16**, 1195–1211.

Wu, R., Z.-Z. Hu, and B. P. Kirtman, 2003: Evolution of ENSO-related rainfall anomalies in East Asia. *J. Climate*, **16**, 3742–3758.

Yasutomi, N., A. Hamada, and A. Yatagai, 2011: Development of a long-term daily gridded temperature dataset and its application to rain/snow discrimination of daily precipitation. *Global Environ. Res.*, **15**, 165–172.

Yhang, Y.-B., and S.-Y. Hong, 2008: Improved physical processes in a regional climate model and their impact on the simulated summer monsoon circulations over East Asia. *J. Climate*, **21**, 963–979.

TABLES AND FIGURES

Table 1. Experimental design

	WRF	GRIMs-RMP	RegCM
Initial & body	CFSR (Saha et al. 2010)		
Dynamical core	Non-hydrostatic	Hydrostatic	Hydrostatic
Convection Parameterization	New SAS (Han and Pan 2011)	SAS (Park and Hong 2007; Byun and Hong 2007)	Emanuel (Emanuel and Zivkovic-Rothman 1999)
Microphysics	WSM3 (Hong et al. 2004)	WSM1 (Hong et al. 1998)	SUBEX (Pal et al. 2000)
PBL	YSU (Hong et al. 2006)	YSU (Hong et al. 2006)	Holtslag PBL (Holtslag et al. 1990)
Land surface	Noah (Chen and Dudhia 2001; Ek et al. 2003)	Noah (Yhang and Hong 2008; Ek et al. 2003)	BATS (Dickinson et al. 1993)

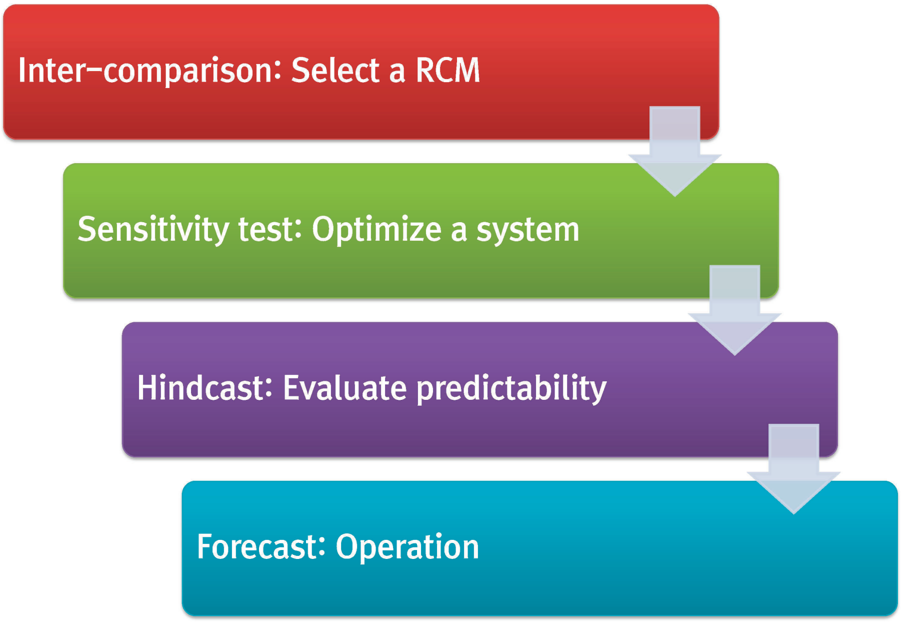

Figure 1. Steps for the APCC-PRePS project.

(a)

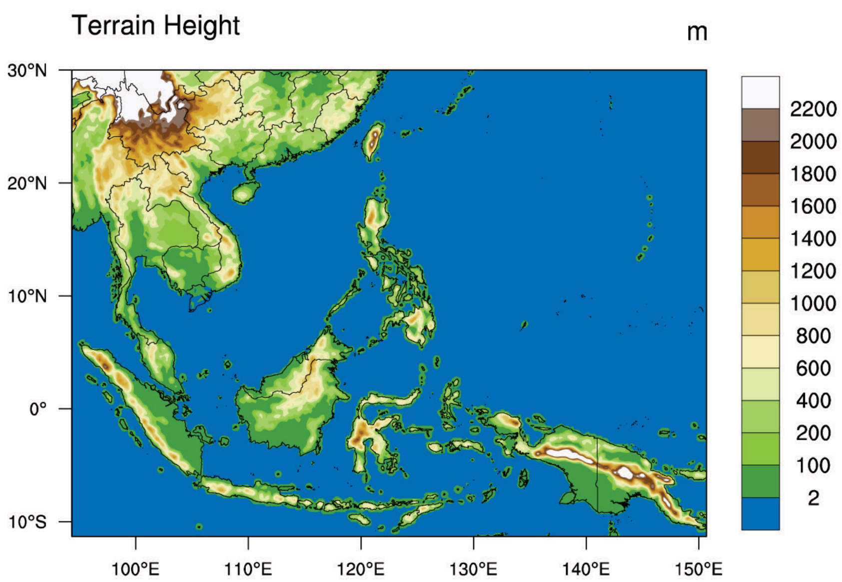

(b)

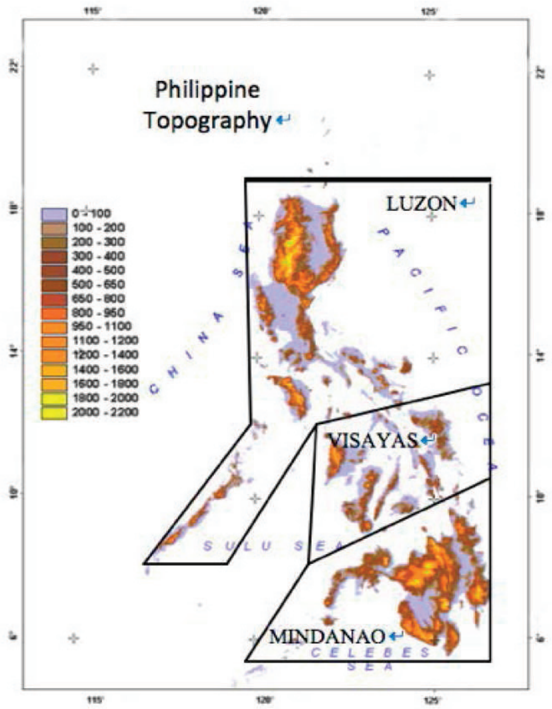

Figure 2. (a) Experimental domain and (b) main islands of the Philippines.

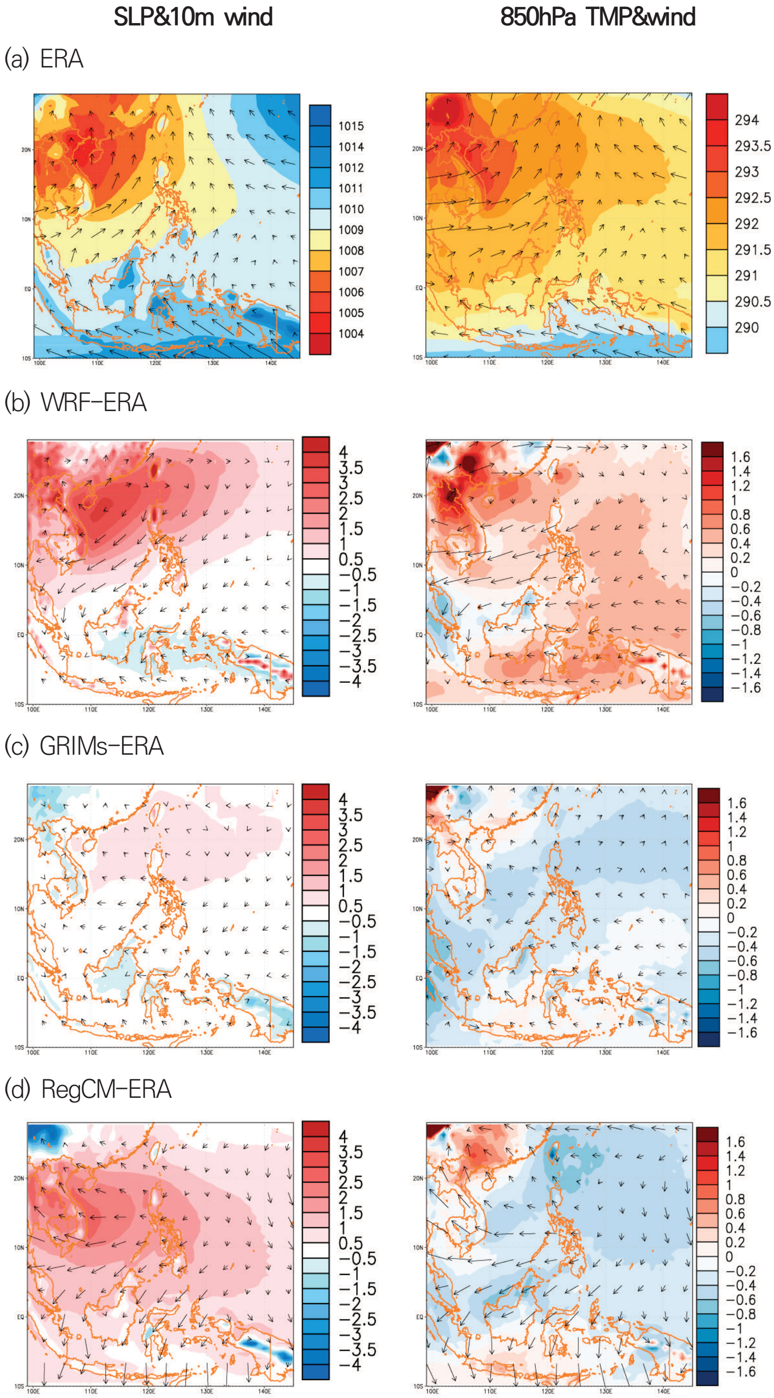

Figure 3. MJJA mean sea level pressure (shaded, hPa) and 10-m wind (vector, m s^{-1}), and temperature (shaded, K) and wind (vector, m s^{-1}) at 850 hPa from (a) ERA-Interim reanalysis and difference between ERA and (b) WRF, (c) GRIMs, and (d) RegCM simulations.

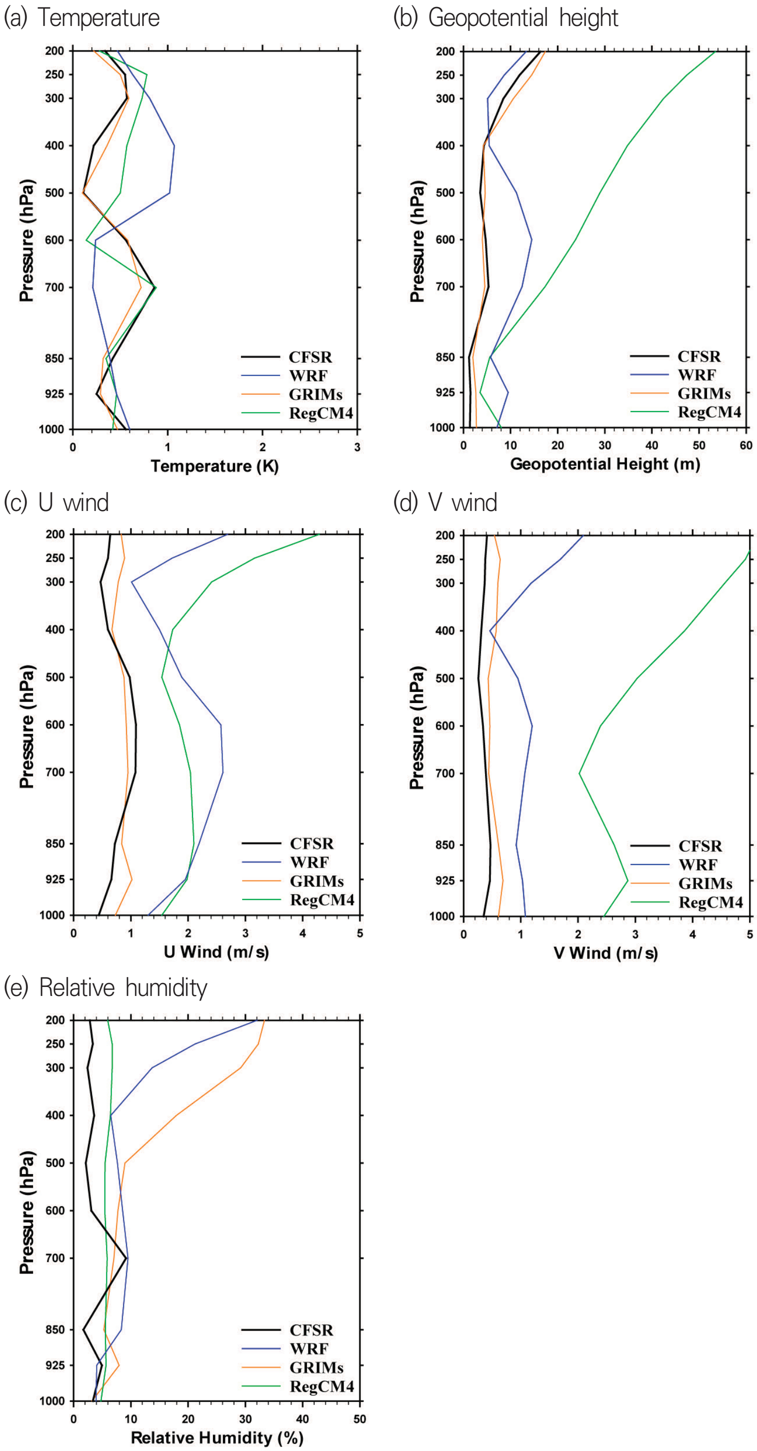

Figure 4. Vertical profile of root mean square error (RMSE) of (a) temperature, (b) geopotential height, (c) relative humidity, (d) zonal wind, and (e) meridional wind.

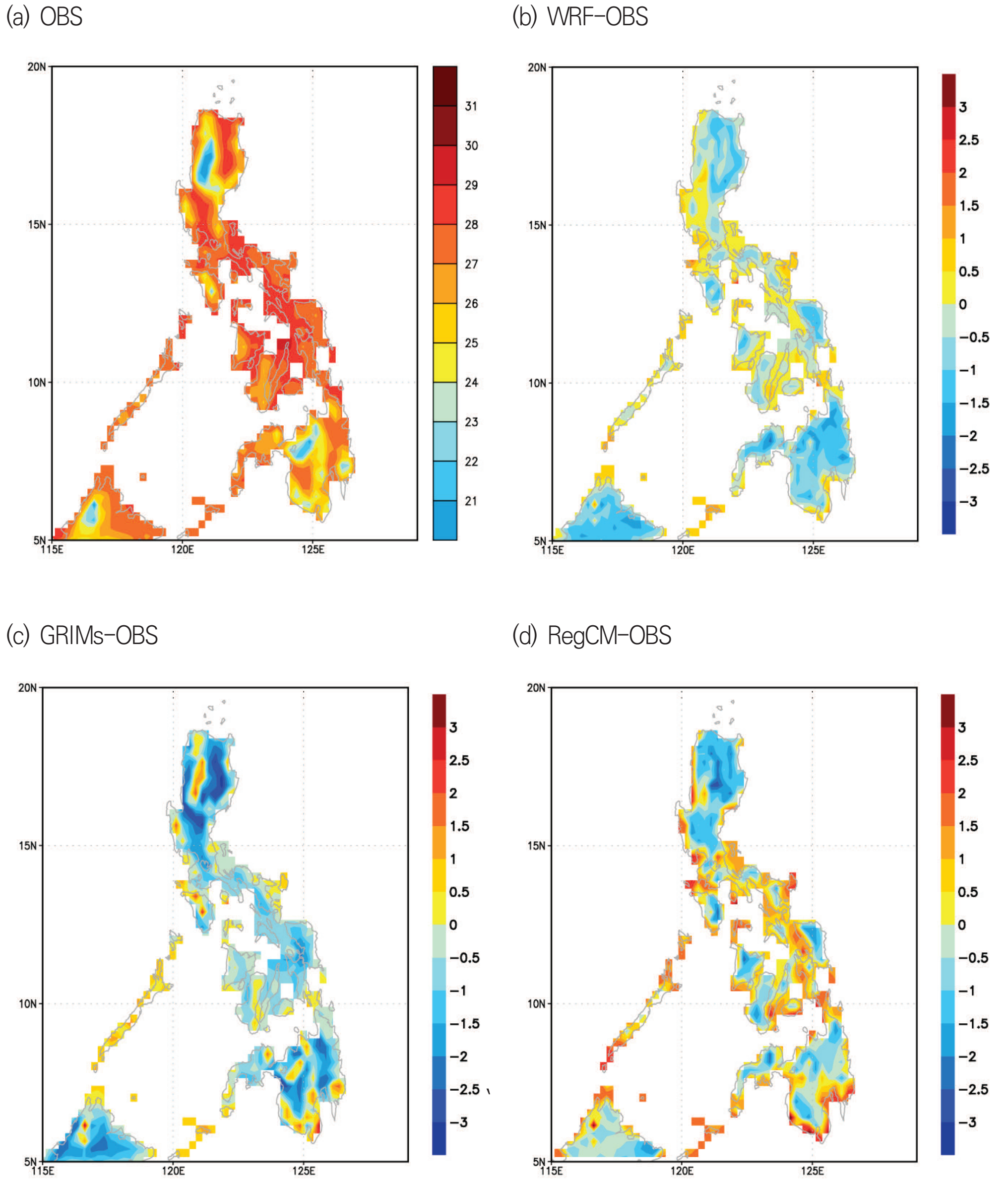

Figure 5. 22-year MJJA surface temperature (°C) of (a) observation, and corresponding difference between observation and (b) WRF, (c) GRIMs, and (d) RegCM simulations.

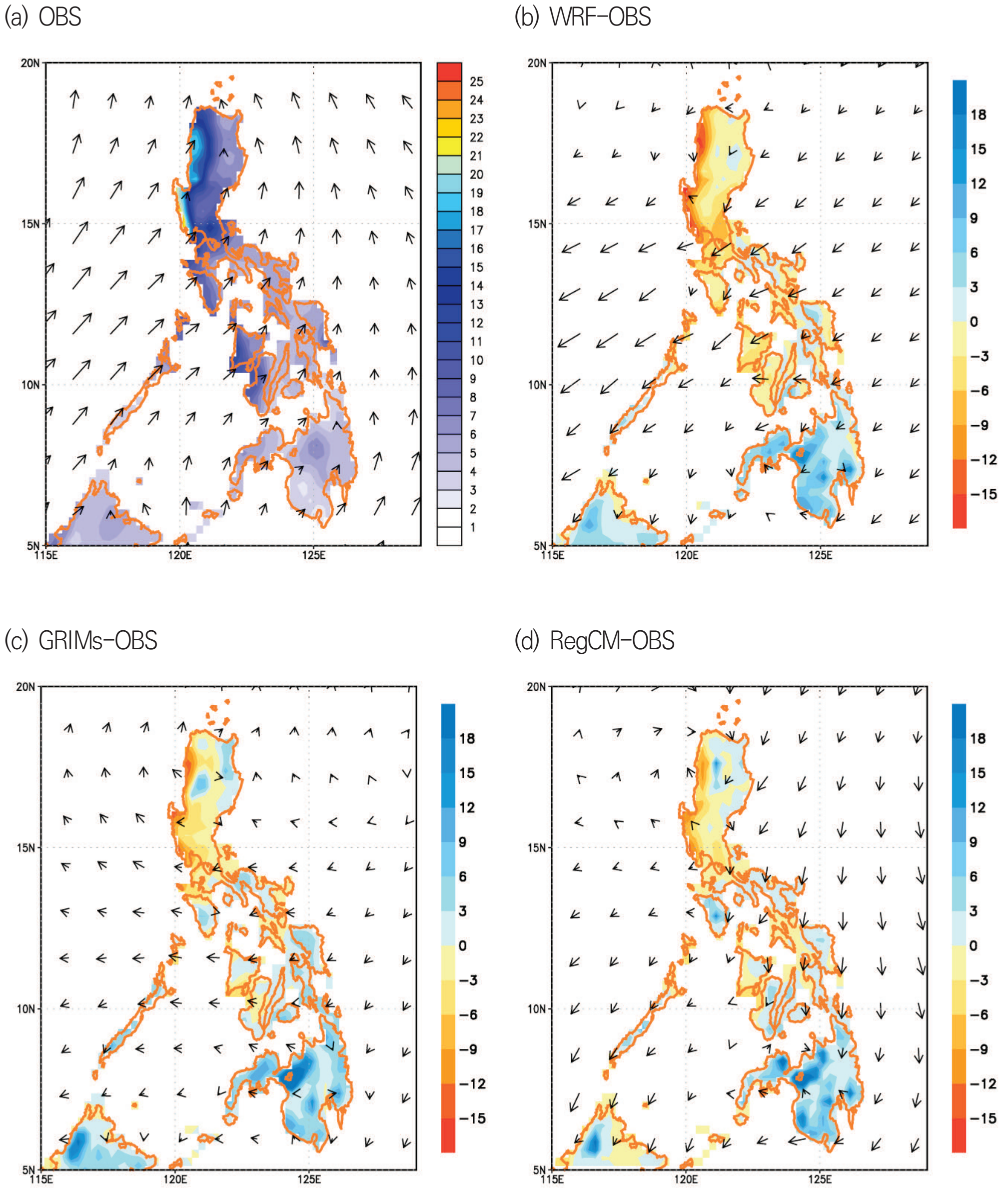

Figure 6. 22-year MJJA precipitation (shaded, mm day^{-1}) and 10-m wind (vector, m s^{-1}) of (a) observation, and corresponding difference between observation and (b) WRF, (c) GRIMs, and (d) RegCM simulations.

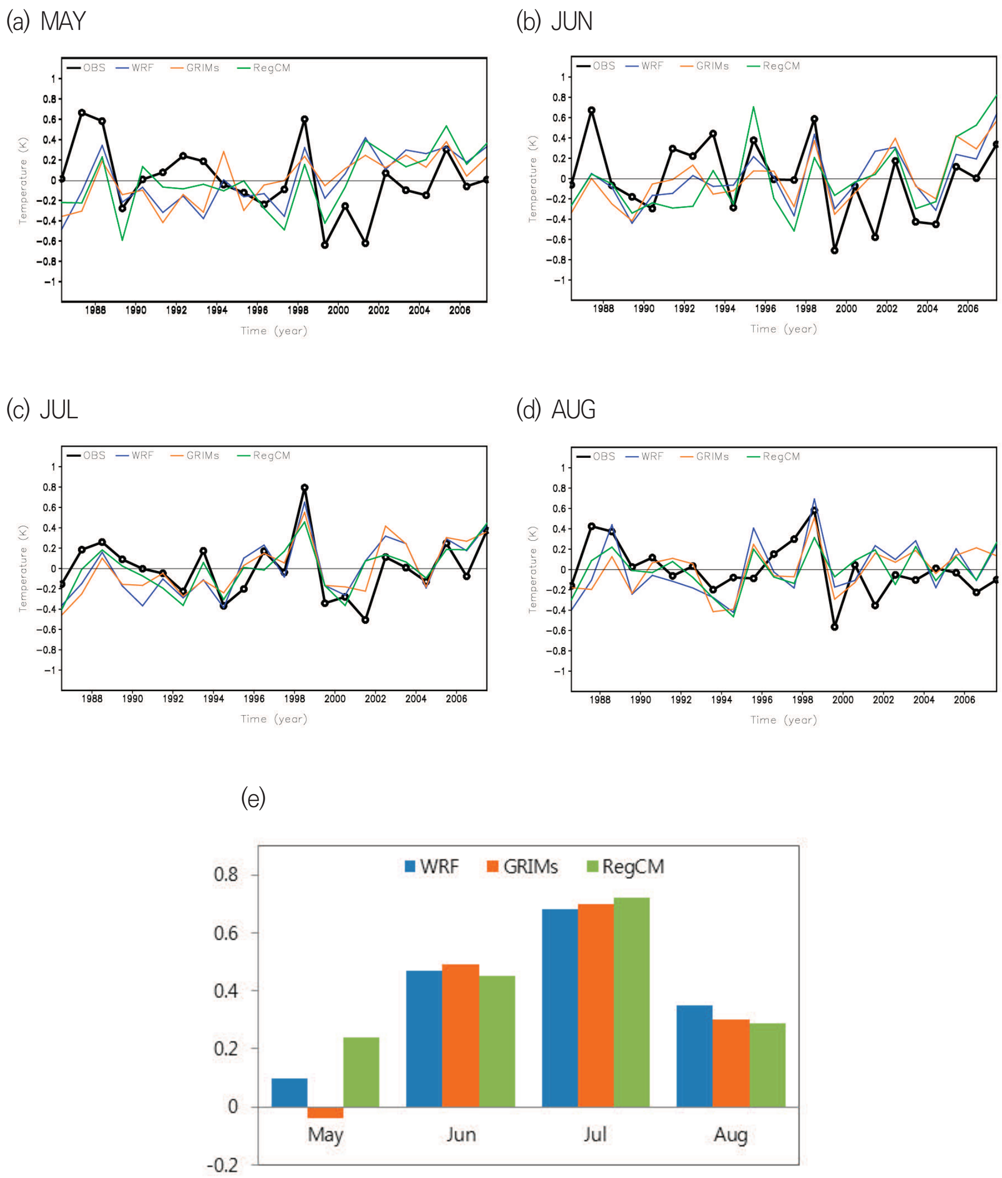

Figure 7. Time-series and temporal correlations of 2-m temperature anomaly averaged over the Philippines for (a) May, (b) June, (c) July, (d) August, and (e) temporal correlation.

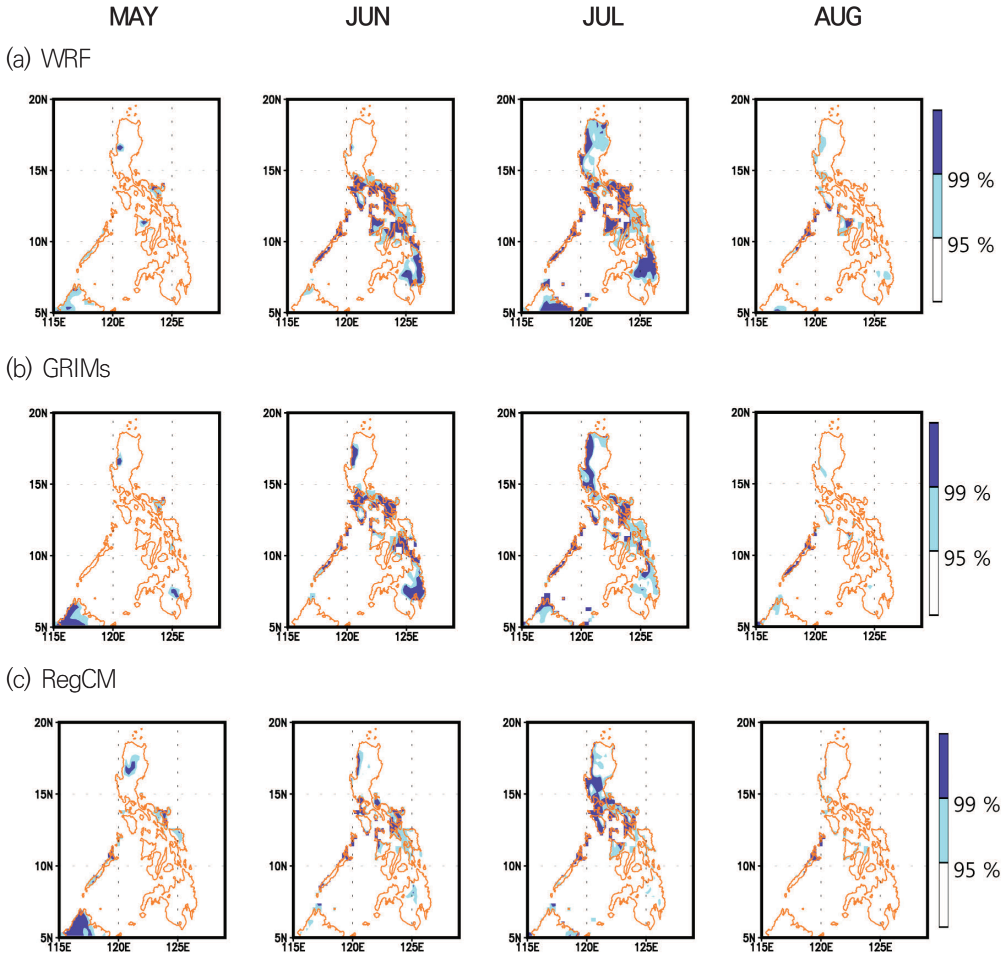

Figure 8. Temporal correlation of 2-m temperature anomaly simulated by (a) WRF, (b) GRIMs, and (c) RegCM during 22 years. Significant values exceeding the 95% (0.444) and 99% (0.561) confidence level (*t* test) are shaded.

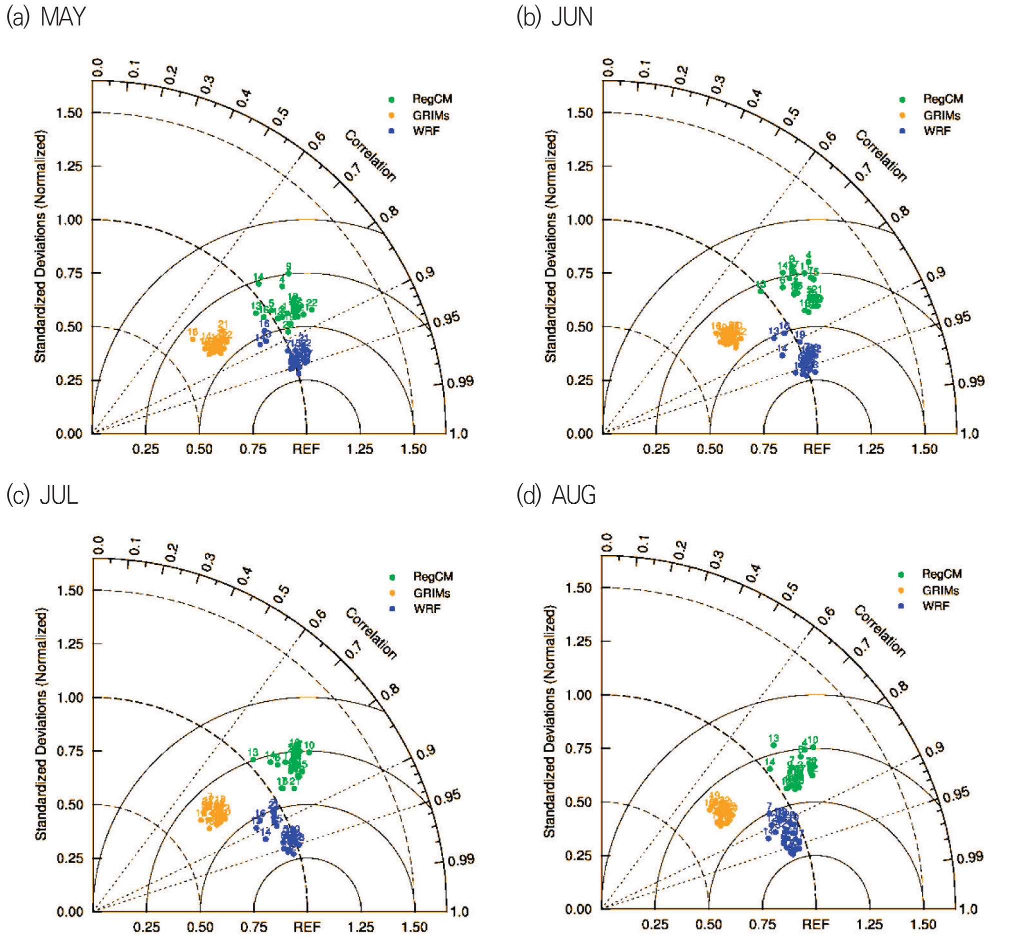

Figure 9. Taylor diagram of simulated 2-m temperature for (a) May, (b) June, (c) July, and (d) August. Spatial correlation and standard deviation for 22 years are calculated. Blue, orange, and green circles are WRF, GRIMs, and RegCM, respectively.

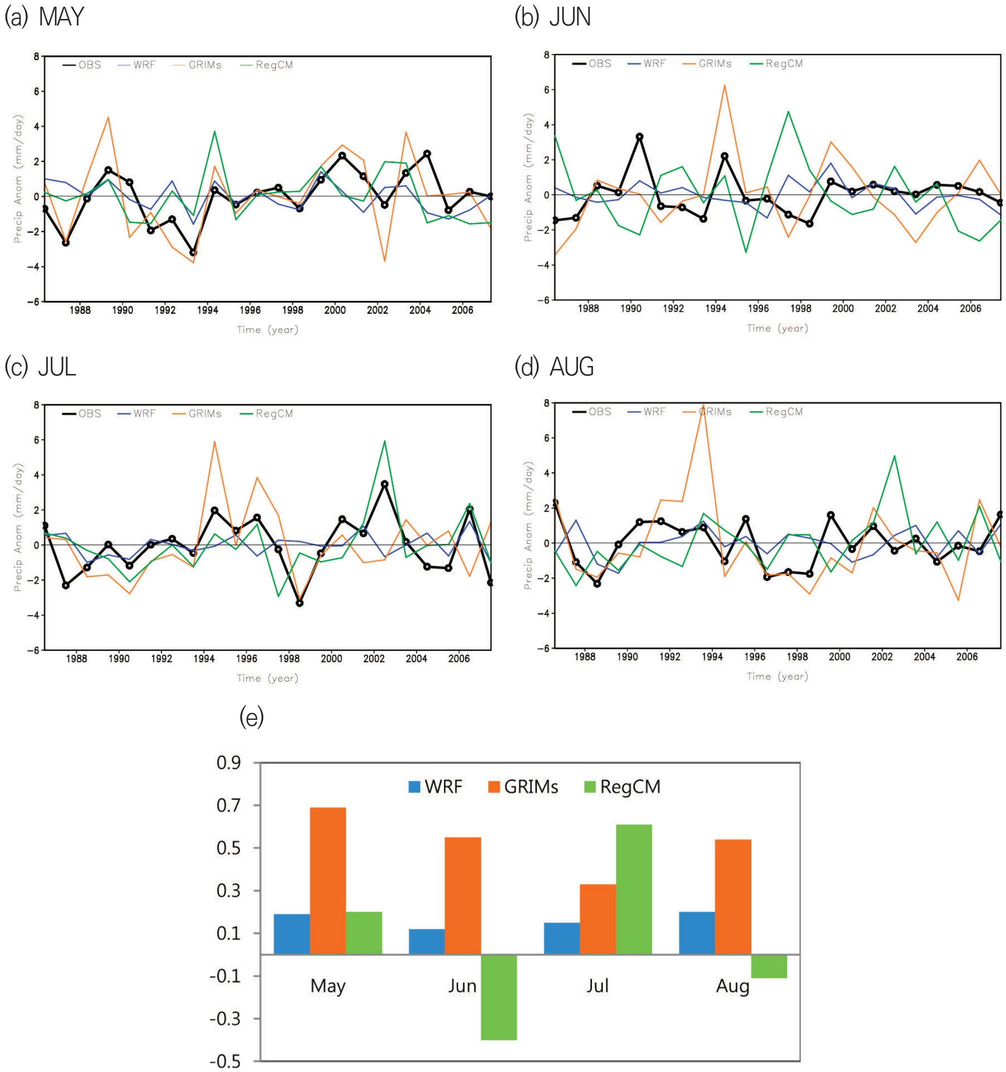

Figure 10. Time-series of precipitation anomaly averaged over the Philippines for (a) May, (b) June, (c) July, (d) August, and (e) temporal correlation.

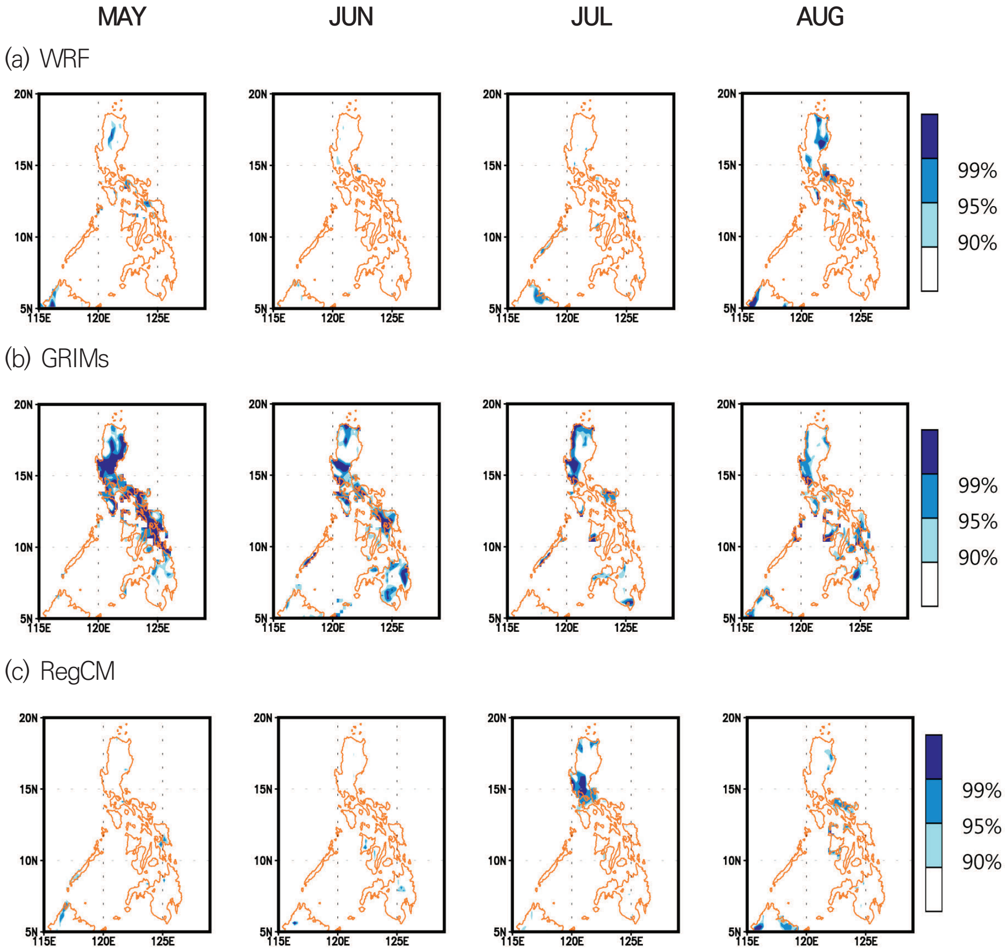

Figure 11. Temporal correlation of precipitation anomaly simulated by (a) WRF, (b) GRIMs, and (c) RegCM during 22 years. Dotted area indicates the 95% significance levels. Significant values exceeding the 90% (0.378), 95% (0.444), and 99% (0.561) confidence level (*t* test) are shaded.

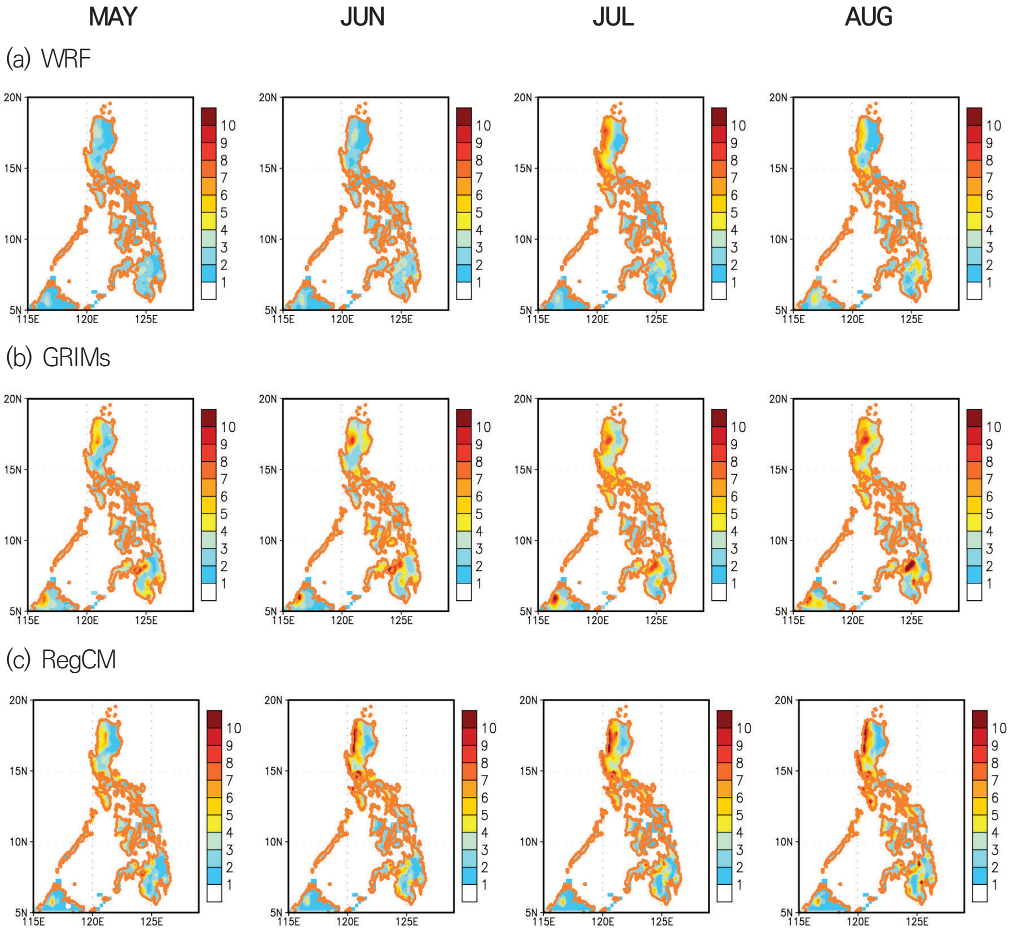

Figure 12. 22-year mean RMSE of precipitation anomaly simulated by the (a) WRF, (b) GRIMs, and (c) RegCM.

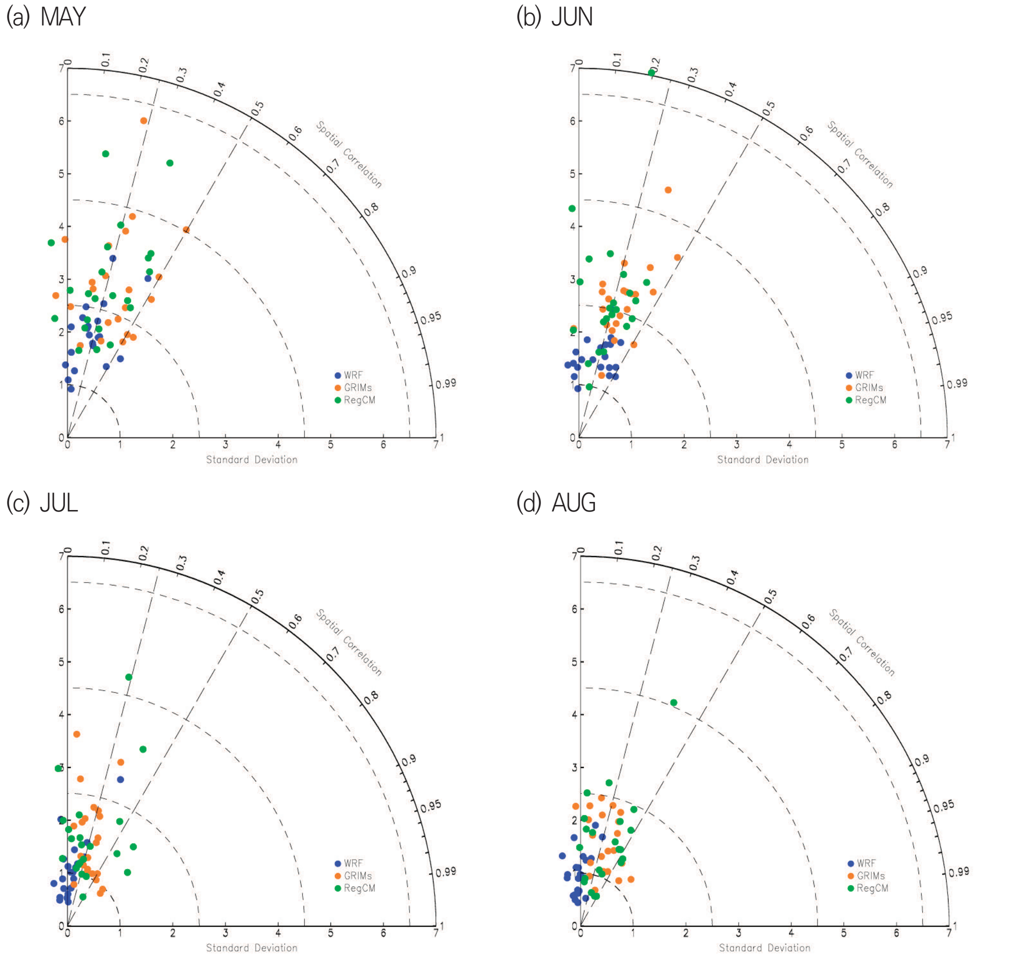

Figure 13. Taylor diagram of simulated precipitation for (a) May, (b) June, (c) July, and (d) August. Spatial correlation and standard deviation for 22 years are calculated. Blue, orange, and green circles are WRF, GRIMs, and RegCM, respectively.

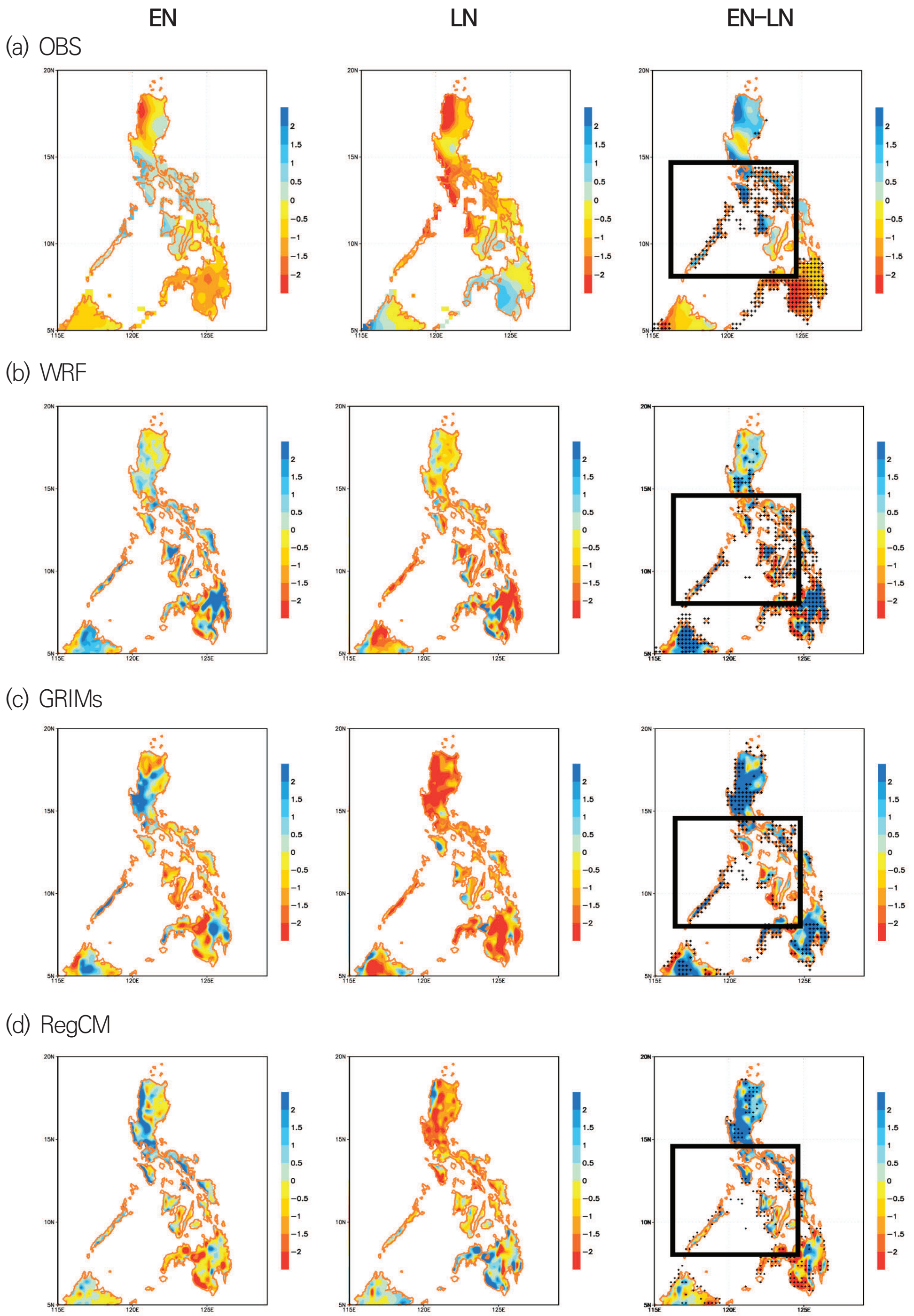

Figure 14. JA (June–July) Precipitation anomalies (mm day^{-1}) of El Niño years (EN; 1987, 1991, 1997, 2002, 2004), La Niña years (LN; 1988, 1998, 1999, 2000), and composite difference (EN – LN). Dotted areas in composite difference indicate statistical significance level (95%).

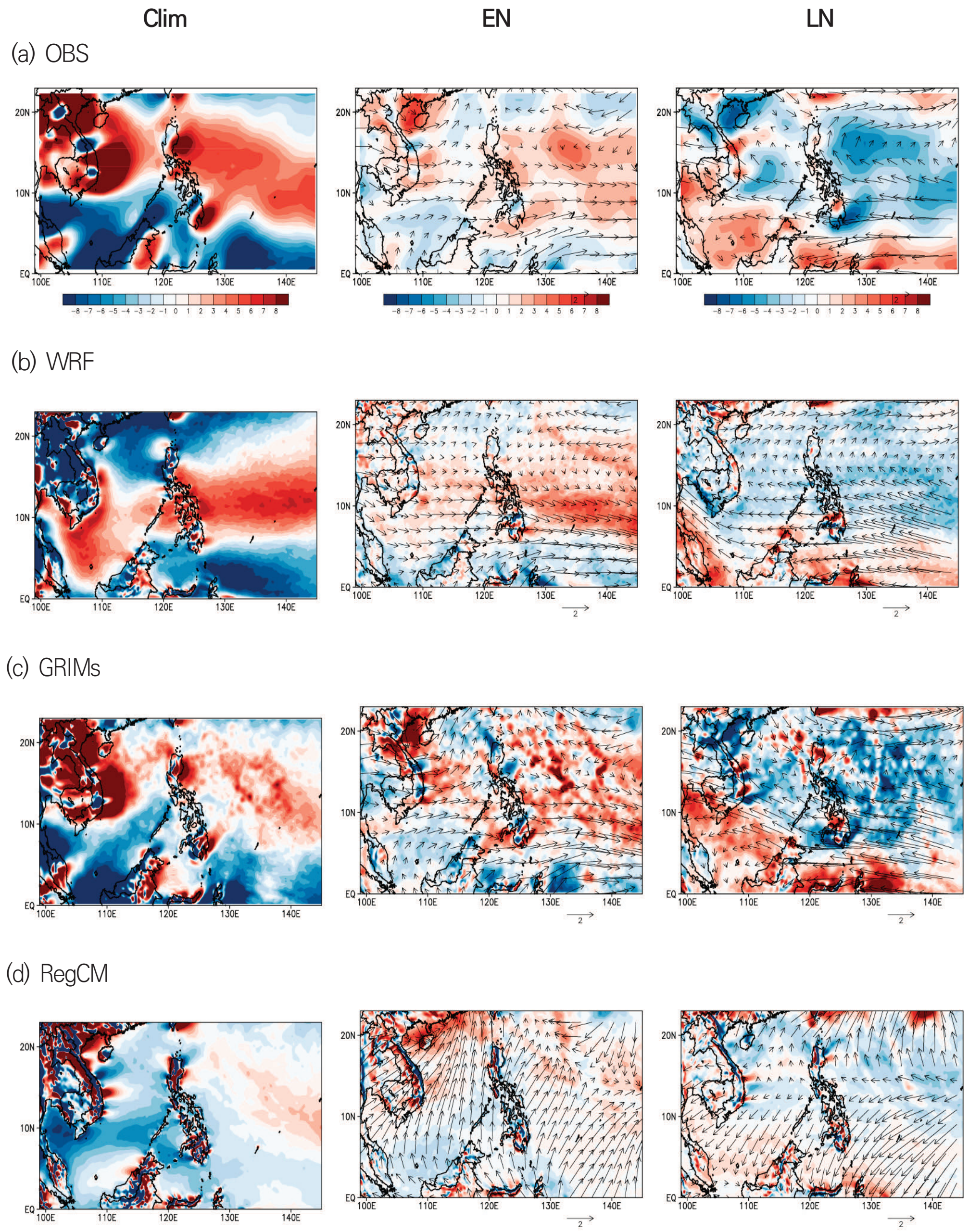

Figure 15. Relative vorticity (shaded, $s^{-1} \times 10^6$) and wind (vector, m s^{-1}) at 850 hPa for July for climatology, and anomalous vorticity for El Niño and La Niña years of (a) ERA-Interim, (b) WRF, (c) GRIMs, and (d) RegCM simulations.

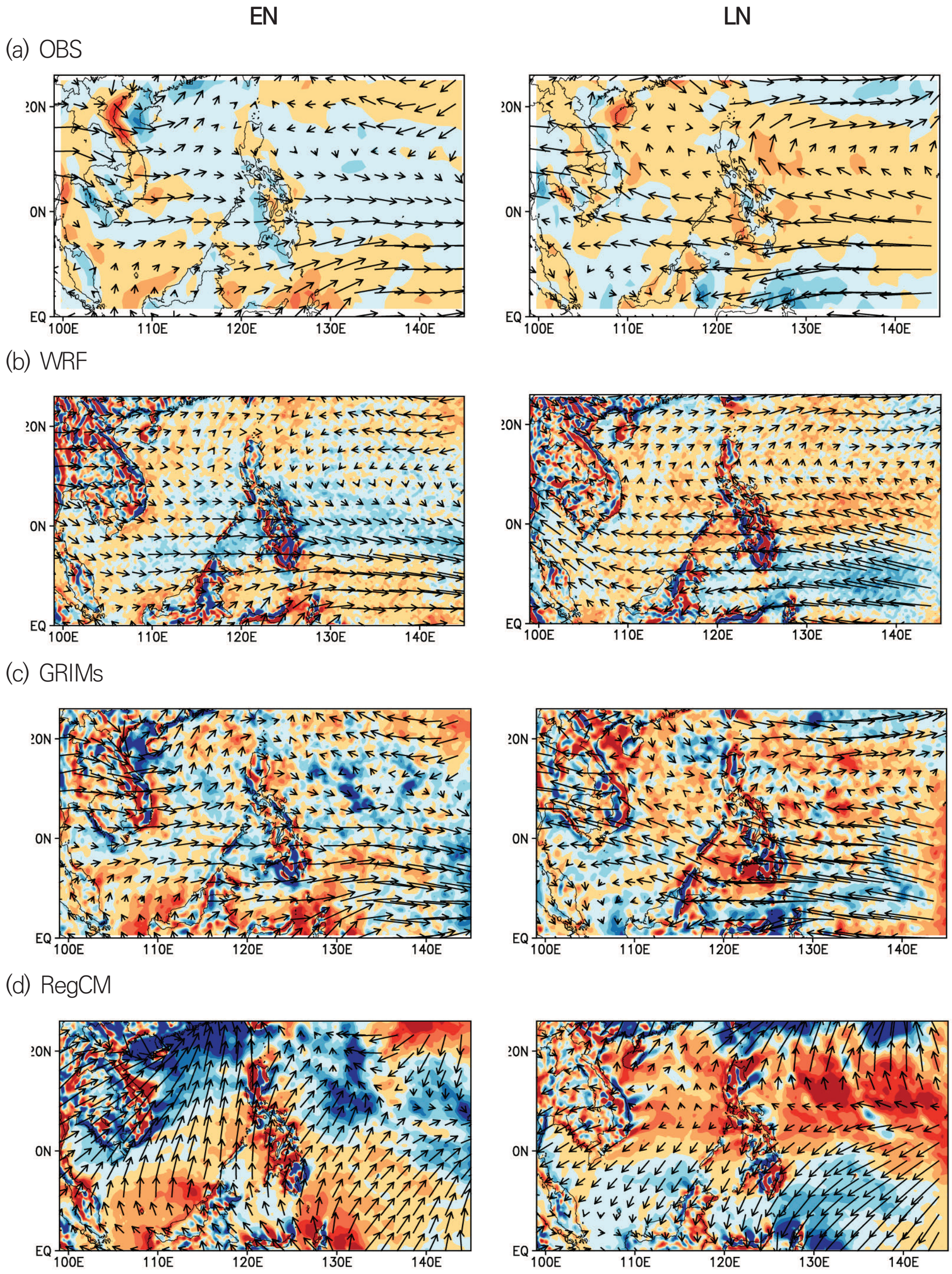

Figure 16. Horizontal moisture flux composite anomalies at 850 hPa (vectors; m s^{-1}) associated with the product of the anomalous wind (q_c) and climatological specific humidity (V_a) and moisture convergence anomalies at surface (shaded; $gk^1 s^{-1}$) during July for El Niño (EN) and La Niña (LN) years of (a) ERA-Interim, (b) WRF, (c) GRIMs, and (d) RegCM simulations. Blue (red) area is convergence (divergence).

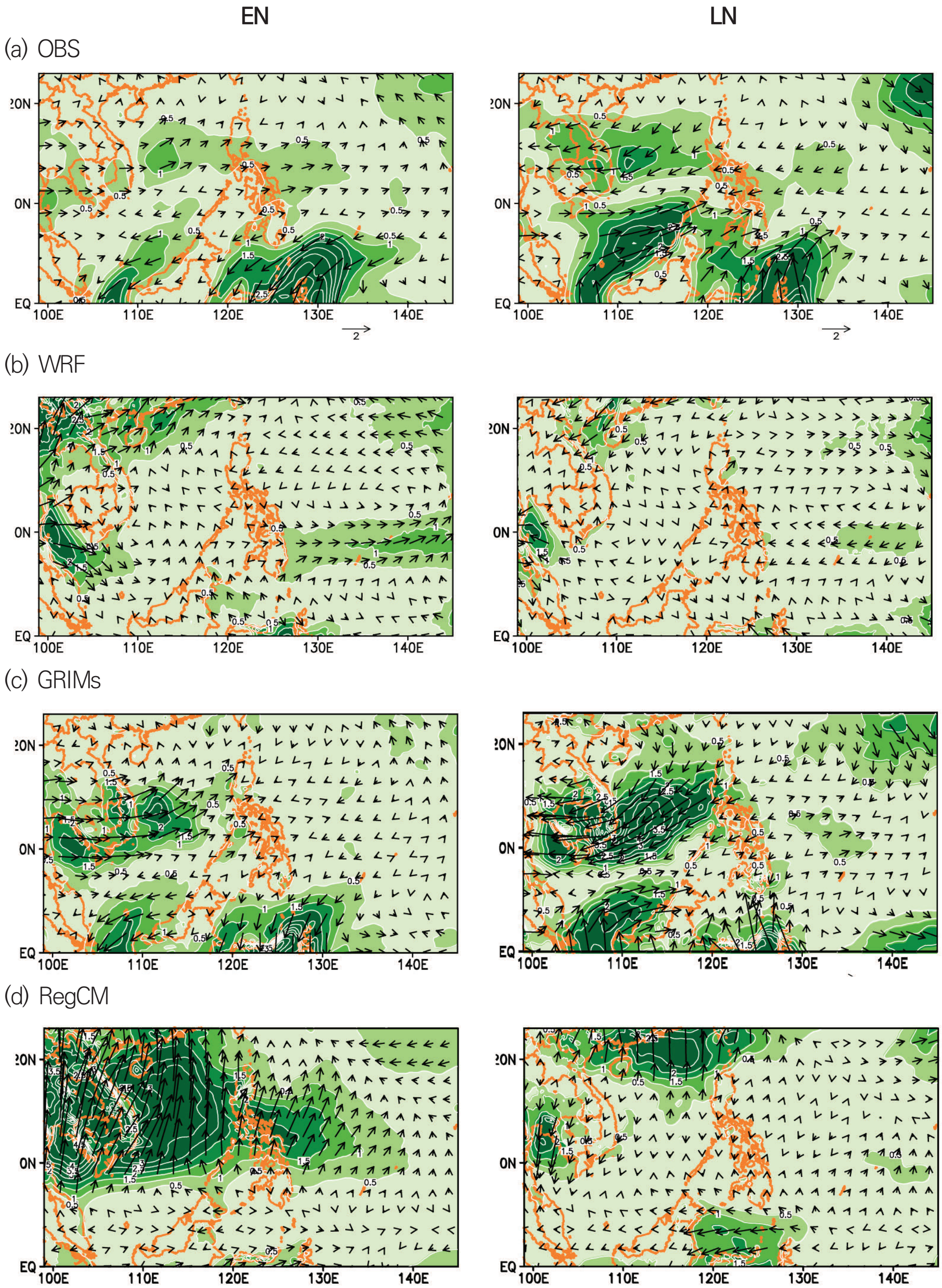

Figure 17. Horizontal moisture flux composite anomalies at 850 hPa (vectors) and their magnitude (shaded; $gkg^{-1}ms^{1}$) associated with the product of the anomalous specific humidity (q_a) and climatological wind (V_c) during August for El Niño (EN) and La Niña (LN) years of (a) ERA-Interim, (b) WRF, (c) GRIMs, and (d) RegCM simulations.

【Research Team】

Yoo-Bin Yhang, Research Fellow

WonMoo Kim, Research Fellow

Chang-Mook Lim, Researcher

Research Report 2017-03

Development of APCC-PAGASA Regional Prediction System (APCC-PRePS) over the Philippines Year 1: Model Intercomparison

ISBN : 979-11-5698-193-0

Published in March 2018

Published by the APEC Climate Center

Produced by Kyungsung Media